Korean J. Chem. Eng., 34(2), 298-304 (2017)
DOI: 10.1007/s11814-016-0290-4

pISSN: 0256-1115
eISSN: 1975-7220

Synthesis and characterization of a K/K_2CO_3-based solid superbase as a catalyst in propylene dimerization

Haibo Jin†, Heng Jiang, Qiwei Wang, Suohe Yang, Guohua Luo, and Guangxiang He†

Department of Chemical Engineering, Beijing Institute of Petrochemical Technology, Beijing 102617, China
(*Received 3 May 2016 • accepted 15 October 2016*)

Abstract−A novel solid superbase $3\%K/K_2CO_3$ was prepared by loading metallic potassium on K_2CO_3. The optimized preparation conditions included a loading time of 1.5 h, loading temperature of 150 °C, loading amount of 3 wt% and average carrier size of 120 μm. Under the optimum conditions, the conversion of propylene is about 60% with the selectivity of dimers 98.5% and the selectivity of 4MP1 86.3%. In addition, the superbase $3\%K/K_2CO_3$ has a base strength of $H_- \geq 37$, and the concentration of basic sites of $H_- \geq 35$ is approximately 0.3 $mmol \cdot g^{-1}_{CAT}$. The microcrystal of metallic potassium was determined using X-ray diffraction (XRD) and differential scanning calorimetry (DSC). It was assumed that the oxygen species, which are adjacent to lattice defects, such as the crystalline corners, edges and vacancies of metallic potassium microcrystals, constituted the superbasic sites.

Keywords: Solid Superbase, Superbasic Site, Base Catalysis, Propylene Dimerization

INTRODUCTION

4MP1 (4-methyl-1-pentene) is an important alpha-olefin that is widely used for copolymerizing linear low density polyethylene (LLDPE). The physical properties of LLDPE, such as tensile strength, impulse strength, and peel strength improve with the carbon atom branch chain of the alpha-olefin, which increases copolymerization [1-3]. Before the 1990s, LLDPE was mostly synthesized industrially by copolymerization ethylene with 1-butene, which is inferior in quality. Now, research has found that replacing 1-butene with many other alpha or branch chain alpha olefins, such as 1-hexene, 1-octylene and 4-menthyl-1-pentene, can produce a superior product. Particularly, LLDPE prepared by copolymerizing with 4MP1 has significantly better physical and chemical properties and a lower cost than C6 or C8 alpha olefin. Additionally, Poly-4MP1 is a thermoplastic resin that possesses amazing properties, such as a low specific gravity, high softening point and high transparence [1]. In recent years, it has become important for many countries to design a suitable process to generate pure 4MP1.

As environmentally friendly catalysts, solid bases have been paid increasing attention for their excellent catalytic selectivities, mild reaction conditions and few disposal problems. Tanabe defined a solid base with a base strength of $H_- \geq 26$ as a superbase [4,5]. The method of alkali metal loading to prepare a solid superbase is effective. Suzukamo produced a solid superbase of $Na/NaOH/\gamma\text{-}Al_2O_3$ by dispersing metallic sodium and sodium hydroxide onto $\gamma\text{-}Al_2O_3$, with a resulting superbasicity of $H_- \geq 37$ [6,7]. Matsuhashi prepared Na/MgO with a base strength of $H_- \geq 35$ and presented a model to generate superbasic sites on MgO [8,9]. It has been proposed that alkali metal is ionized to form an alkali cation and that the released electron from the alkali metal is trapped in oxygen vacancies to form F^+ centers or F centers. The F^+ centers or F centers donate the electron to nearby O^{2-}, increasing the electron density of O^{2-}. The O^{2-} ions near the F^+ or F centers are super-basic sites [4,8,9]. However, some studies reported that when the loading amount of alkali metal increased or the surface properties changed, the alkali metal was found on the resulting catalyst and acted as the active species [4].

Bota impregnated mesoporous $\gamma\text{-}Al_2O_3$ with methanol solutions of sodium azide and subsequent decomposed azide to obtain a catalyst, which was denoted as $NaN_3/MSU\text{-}\gamma 84$. Furthermore, metallic sodium particles were found in the catalyst by using ^{23}Na MAS NMR and were believed to be related to the basicity [10]. Martens impregnated NaN_3 onto zeolites Y and distinguished three different sodium species in sodalite cages using ESR spectroscopy: extralattice Na^0_x, intracrystalline Na^0_y clusters and ionic Na^{3+}_4 clusters. It was suggested that the framework oxygen anions in the neighborhood of intra-crystalline metallic clusters acted as the active sites [11]. Nozue exposed low-silica X (LSX) to metallic sodium vapor to prepare Na_n/Na_{12}-LSX (n=1 to 12). A drastic decrease in resistivity was observed at $n \approx 12$, which can be attributed to the fundamental change in the size of the metallic sodium particle [12,13].

In 1961, Schramm first proposed that solid base catalysts prepared by dispersing alkali metal on carbon potassium had a high activity regarding the dimerization of propylene to iso-hexene [14] to produce high octane iso-hexene additives for gasoline. One iso-hexene, in particular, 4MP1, can also be used to copolymerize LLDPE to obtain a superior product. Thus, the design, preparation and employment of such a catalyst became the objective of many researchers [1,14,15]. The propylene dimerization reaction has been performed in different reactors (autoclave and fix-bed) in the presence of the solid superbase studied by Schramm. It resulted in a 62% conversion by weight, 78% selectivity to hexene in the autoclave reactor and 80% selectivity to hexene in the fixed-bed reactor [1]. Wilkes stated that the metal particle size dispersed on the carrier

†To whom correspondence should be addressed.
E-mail: jinhaibo@bipt.edu.cn, hgx@bipt.edu.cn
Copyright by The Korean Institute of Chemical Engineers.

surface had a great influence on the final catalytic activity. The catalyst was implemented in a bubble column with a conversion limited to 10% per pass, reaching 81% selectivity to 4MP1 [2,16-18]. In 1968, Hambling first applied a solid superbase catalyst to industrial operation, producing products with 87.1% selectivity to 4MP1 [19-21]. According to data from the Phillips Petroleum Company, in 1986 [22], catalysts prepared by adding extra template and agent were implemented in a fix-bed reactor under optimized conditions, producing products with approximately 22.6% conversion to hexene by weight and 89% selectivity toward 4MP1. In 1991, the company disclosed that another catalyst used a compound comprising alkali metal salt and Al_2O_3 as a carrier was implemented in a fix-bed reactor producing products with approximately 27% conversion to hexene by weight and 86% selectivity to 4MP1 [23-25]. Catalysts prepared by dispersed alkali metal on a novel carrier $K_2O{\cdot}xAl_2O_3$ ($0.5\leq x\leq 11$) exhibited high activity in propylene dimerization [25]. Such catalysts were implemented in an autoclave reactor for 8 h, forming products with approximately 55% conversion to hexene by weight and 89% selectivity to 4MP1. Zhang et al. dispersed alkali metal on carbon potassium with a pore volume 0.1 ml/g and a pore diameter of 100 nm. The catalyst was implemented in a flow reactor, producing products with approximately 32% conversion to hexene by weight per pass and 90% selectivity to 4MP1 [26].

The mechanism of the solid superbases catalyzing the dimerization of propylene is the foundation of synthesizing the product 4MP1. According to the research of Shaw, there are three steps in dimerization of propylene to 4MP1 in the presence of a solid superbase. First, propylene is adsorbed on the surface of the catalyst, producing an active intermediate, potassium allyl. Second, potassium allyl combines with propylene, generating a 4-methyl-1-pentene anion. Third, the 4-methyl-1-pentene anion combines with another propylene to generate the product and a new potassium allyl [15,27]. Because the affinity between propylene and the intermediate is stronger than between propylene and 4MP1, a tripolymer or high polymer of propylene is not likely to be produced during the reaction. Because of polarization, 4MP1 is easily transformed into 4-methyl-2-pentene (4MP2), 2-methyl-2-pentene (2MP2), and so on. Therefore, reducing the contact time between propylene and the catalyst and decreasing the reaction temperature might help to increase the selectivity of the dimerization reaction of propylene to 4MP1 [19].

The novel solid superbase of K/K_2CO_3 catalyzed the dimerization of propylene to 4MP1 with high selectivity. The modification abilities of the catalyst have been extensively studied, but the formation mechanism of the surface of superbasic sites is not fully understood [16,20,28]. In this paper, we systematically studied the preparation conditions of the catalyst (loading time, loading temperature, metal loading amount and carrier size). The characterization methods of titration with Hammett indicators, XRD, DSC and H_2-TPR were used to investigate the formation mechanism of super basic sites.

MATERIAL AND METHODS

1. Preparation and Probe Reaction of the Catalyst

1-1. Preparation of the Catalyst

The catalyst was prepared by first stir-drying 0.1 g of talc with 10 g of potassium carbonate (produced by Guangfu Fine Chemical, Tianjin, China) of a certain average particle size (carrier size), which was selected by using a specific mesh sieve, at 380 °C for 2 h in a nitrogen gas atmosphere in a three-necked flask. The temperature was then decreased to 90-210 °C (loading temperature), and 1-5 wt% potassium with potassium oxide excised from the surface (produced by Aladdin, America) was loaded by weight of potassium carbonate (metal loading amount). After 0.5-3.5 h of stirring (loading time), the resulting catalyst was stored in 30 mL of n-hexane and charged to a 100-mL autoclave (produced by Parr Ltd., America), with 5.00 mL of n-heptane as the internal standard for quantitative GC analysis. At this point, the mass of the autoclave, m_1, was determined (±0.25 g).

1-2. The Probe Reaction of Catalysis

For the probe reaction, 27 g (±0.25 g) of propylene was added to a 100-ml autoclave to obtain an initial pressure of 0.75 MPa in the reactor. The dimerization was performed at 150 °C for 20 h, with the highest reaction pressure in the autoclave reaching 5.5 MPa. At the end of the reaction, the autoclave was quenched to a temperature below −5 °C so that the dimers could completely liquefy, which reduced the variability of this experiment. The gas phase, which was directly vented, consisted of less than 1 wt% dimer and more than 95 wt% of propylene. The mass of the autoclave with the liquid phase, m_2, was weighed (±0.25 g). The liquid phase was sampled and subjected to GC analysis to determine the amount of the 4MP1 product, m_{4MP1}; propylene not reacted, m_{prop}; and dimers, m_{dimer}, which includes 4MP1, 4MP2, 1-hexene (1-Hex), and other hexenes. According to the experimental data, the average speed of the reaction can reach $0.062\ g_{prop}{\cdot}g^{-1}_{CAT}{\cdot}h^{-1}$. Because of its instability, 4MP1 it can easily transfer into 4MP2 or other isomers. The speed of isomerization can reach $0.016\ g_{4MP1}{\cdot}g^{-1}_{CAT}{\cdot}h^{-1}$. Moreover, the isomerization activity increases with the reacting temperature, the loading amount of alkali metal and the surface area of the carrier escalated.

1-3. Calculation of the Composition of Product

Quantitative GC analysis was performed using the internal standard curve method. The type of GC instrument used was a GC14C (produced by Shimadzu, Japan) equipped with a flame ionization detector (FID) and a 50 m HP-5MS glass capillary column.

The conversion of propylene is defined as X, $X=\dfrac{m_2-m_1}{27}\times 100\%$

The selectivity of dimers is defined as S_1, $S_1=\dfrac{m_{dimer}}{m_2-m_1}\times 100\%$

The selectivity of the desired product, 4MP1, is defined as S_2,

$S_2=\dfrac{m_{4MP1}}{m_{dimer}}\times 100\%$

The catalysts in the dimerization process require a long time to exhibit their full activities. This time is defined as the inducing period, $t_{inducing}$, the time elapsed when the decrease in the reaction pressure reaches 5% of the highest pressure during the reaction.

2. Catalyst Characterization

2-1. Determination of the Base Strength

The base strength was measured by titration using Hammett indicators. The indicators were biphenyl methane (H_-=35) and isopropyl benzene (H_-=37). A catalyst sample of 1 g was sealed by using n-hexane and was subsequently charged to a three-necked

flask into which several drops of indicator were also added. The mixture in the flask was heated and stirred at reflux until its color changed. Benzoic acid, dissolved in n-hexane at a concentration of 0.05 mol·L^{-1}, was gradually added dropwise into the flask through a pressure-equalizing dropping funnel. When the color changed visibly again, the amount of consumed benzoic acid was measured to calculate the amount of basic sites.

2-2. Measuring Condition of the XRD

The XRD patterns of the samples were recorded on an XRD-7000 (produced by Shimadzu, Japan) with Cu-Kα radiation, an acceleration voltage of 40 kV and a current of 20 mA. Data were collected at 2θ over a range of 20 to 50° with a scanning speed of 1°·min^{-1}.

2-3. Measuring Condition of the DSC

Differential scanning calorimetry (DSC) experiments were performed in a meter R20 thermal-analyzer (produced by TA Instruments, America). Under a nitrogen atmosphere, approximately 10 mg of the sample was heated in an alumina crucible at a rate of 5 °C·min^{-1} from 20 °C to 70 °C.

2-4. Measuring Condition of the H_2-TPR

The H_2-temperature reduction (H_2-TPR) test was performed in a CHEMISORB-2750 chemical adsorption instrument (produced by Micromeritics, America). Under a stream of carrier gas (N_2), approximately 0.1 g of sample was heated to 200 °C at a rate of 15 °C·min^{-1} and maintained for 1 h, after which it was cooled to room temperature. Then, the stream changed to adsorbent gas (10% of H_2 and 90% of Ar) at a flow rate of 20 mL·min^{-1}. After that, the signal of the thermal conduction detector (TCD) became stable, the sample temperature increased to 500 °C at a rate of 10 °C·min^{-1}, and the H_2-TPR curve was obtained.

RESULTS AND DISCUSSION

1. Catalyst Characterization

1-1. Surface Basicity Determination

The samples in the basicity determination were prepared at 150 °C for 1.5 h with 3 wt% metal potassium, which was loaded on potassium carbonate with an average particle size of 120 μm and labeled as 3%K/K_2CO_3. The catalyst samples were able to change the color of isopropyl benzene (H_-=37) from colorless to pink; therefore, the highest base strength of H_-≥37 was denoted. The basic site concentration of H_-≥35 was 0.3 mmol·g^{-1}_{CAT}. The base strength was sufficiently high to abstract the α-H of propylene (H_-≈35) to form the active intermediate potassium allyl [13,29]. The potassium allyl is an important active intermediate. The catalyst, as prepared, could abstract the α-H of propylene to form potassium allyl, and then, potassium allyl could easily combine with propylene to generate 4MP1. Generally speaking, the process of forming potassium allyl always was the controlled step.

1-2. XRD Characterization

Fig. 1 shows the XRD patterns of K/K_2CO_3. In the patterns of D, new diffraction lines appeared with 2θ values of 23.6° and 33.6°, which were assigned to the crystal phase of metal potassium. When the loading amount of metal potassium increased to 5 wt% in sample E, the peak intensity of metal potassium was obviously enhanced. The results show the existence of a crystal phase of metal potassium on the catalyst. The close-packed monolayer model was used to calculate the dispersion threshold of metal potassium on potassium carbonate. The calculated threshold was approximately 7 wt%, which was higher than the result of the XRD patterns (less than 3 wt%) [30,31]. This difference indicates the low utilization of the specific surface area of the carrier. The dispersion of metal potassium on potassium carbonate was assumed to be incorporated into specific sites, such as the crystal vacancies in the carrier.

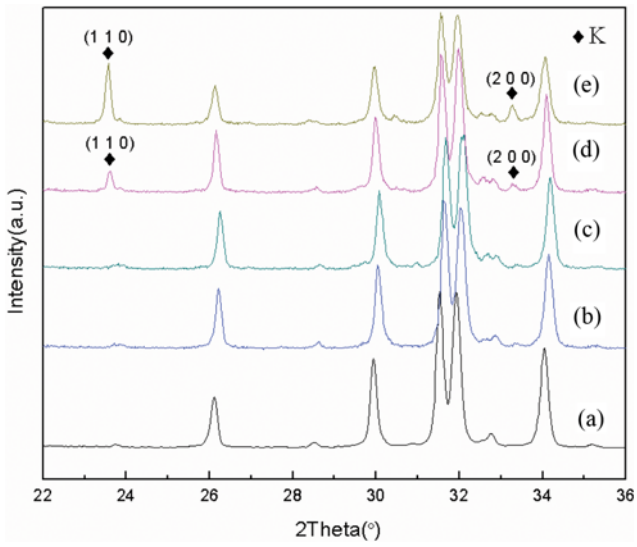

Fig. 1. XRD patterns of catalysts with increment in metal potassium loading amount ((a) K_2CO_3, (b) 1.5%K/K_2CO_3, (c) 2.2%K/K_2CO_3, (d) 3%K/K_2CO_3, (e) 5%K/K_2CO_3; Samples were prepared at 150 °C for 1.5 h with carrier of 120 μm).

In Fig. 2, the characteristic peaks of metal potassium in samples B, C and D weakened, which indicates a loss of metal potassium in the catalyst. This loss is the main reason for catalyst deactivation. Furthermore, the dispersion of potassium oxide is different

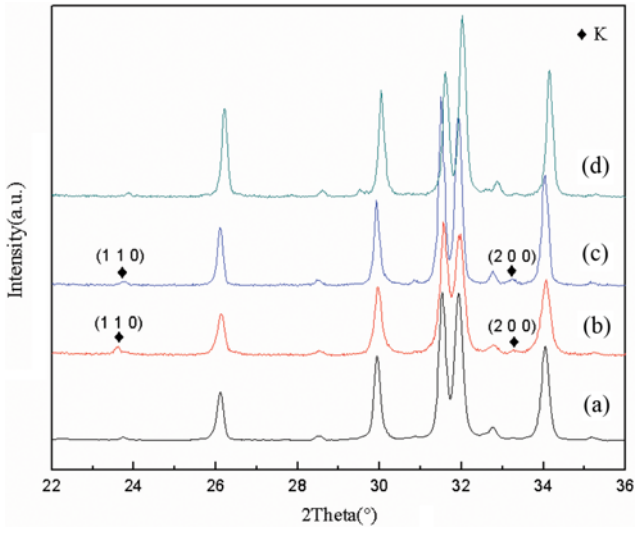

Fig. 2. XRD patterns of partially inactivated catalysts ((a) carrier, (b) catalyst 3%K/K_2CO_3, (c) catalyst used twice, (d) 3%K/K_2CO_3 oxidized by air for 4 h).

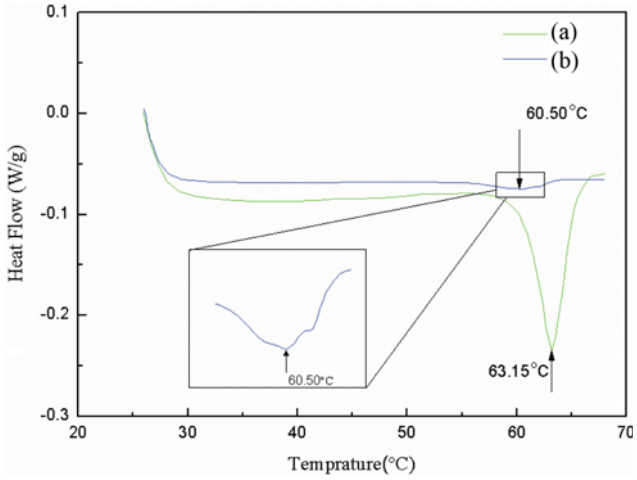

Fig. 3. DCS Curves of catalysts ((a) metal potassium lump, (b) catalyst 3%K/K_2CO_3).

from that of metal potassium because there is no characteristic peak of potassium oxide in the pattern of D, which had an identical loading amount of metal potassium as sample B.

1-3. DSC Characterization

Fig. 3 shows the DSC curves of metallic potassium lumps and the catalyst 3%K/K_2CO_3. In Fig. 3(a), there is one endotherm centered at approximately 63.1 °C, which is the standard melting point of potassium metal. Additionally, one endotherm appears in (b), which corresponds to the fusion of potassium metal. The endotherm in (b) is centered at approximately 60.5 °C, which is 2.7 °C lower than in (a). Thus, the catalyst has a larger specific area ratio and better dispersion of crystalline potassium metal, which results in a higher catalytic activity for K/K_2CO_3 than for the potassium lump.

1-4. H_2-TPR Characterization

The H_2-TPR method was used to characterize oxygen species

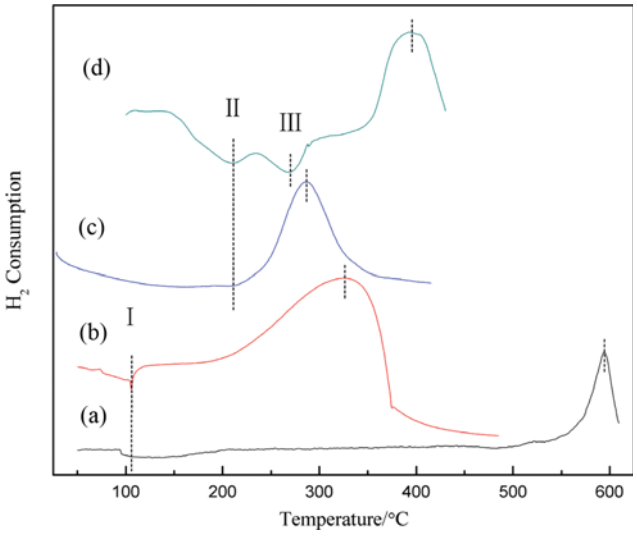

Fig. 4. H_2-TPR test curve ((a) carrier after heat treatment, (b) K metal lump, (c) 3%K/K_2CO_3 oxidized by air for 4 h, (d) fresh catalyst 3%K/K_2CO_3).

in the catalyst. The basic sites are thought to consist of oxygen species. However, the type of oxygen species that constitute the superbasic sites on K/K_2CO_3 has not been determined. In the H_2-TPR curves of Fig. 4, there are both negative peaks due to hydrogen desorption and positive peaks due to hydrogen consumption because of the reduction of oxygen species. The reduction peak of sample (A) is centered at 580 °C, which is directly assigned to the reduction of lattice oxygen in crystalline potassium carbonate. The reduction peaks of samples (B), (C) and (D) are at 325 °C, 295 °C and 380 °C, respectively, with a temperature sequence of D>B>C, which reveals various electron characteristics. Moreover, the reduction peaks of (B) and (D) significantly broadened, which indicates the diverse oxygen species in the samples. The reduction peak of sample (C) can be assigned to the reduction of oxygen species in the highly dispersed microcrystals of potassium oxide on the carrier. The hydrogen desorption peaks can be categorized into three types, labeled I, II and III. I can be assigned to physical adsorption, whereas II and III belong to the chemical adsorption of two different patterns. Practically, II can be related to crystalline potassium oxide. Therefore, III can be related to the superbasic sites. It has been suggested that the superbasic sites on K/K_2CO_3 are oxygen species, which are adjacent to lattice defects, such as the crystalline corners, edges and vacancies on the surface of metal potassium microcrystals, which are highly dispersed on the carrier [4]. The oxygen species should exhibit higher electron density because of electron donation from potassium metal microcrystals, which increases the ability to donate electron pairs and abstract hydrogen protons to form superbasic sites [10-12]. The properties of the oxygen species in samples B and D should be similar because both samples can catalyze the dimerization of propylene. However, D has a far higher conversion than B, which possibly results from the great disparity in the amount of superbasic sites.

2. Discussion of the Catalyst Preparation Conditions

The studied catalyst preparation conditions include loading temperature, loading time, metal loading amount and carrier average size. The loading process of potassium metal on a carbonate potassium carrier can be divided into three periods, nucleation, microcrystal growth, during which the amount of microcrystals increases, and equilibrium crystal formation, during which the microcrystals gradually coalesce [29].

2-1. Effect of the Loading Time

Fig. 5 demonstrates the effect of the loading time on the conversion (X), inducing period ($t_{inducing}$), dimer selectivity (S_1) and 4MP1 selectivity (S_2). In Fig. 5, the maximum X and minimum $t_{inducing}$ both occurred in the scope of the experiments. However, S_1 and S_2 did not show any notable variations. During preparation of the K/K_2CO_3 catalyst, three periods (nucleation, microcrystal growth and equilibrium crystal formation) emerge during which the size of the surface microcrystal continuously increases, wherein its quantity first increases and subsequently decreases from a maximal value. The results of X in (A) and $t_{inducing}$ in (B) of Fig. 5 are generally consistent with the changes in the quantity of the surface microcrystal, which is related to the amount of surface basic sites. Moreover, small changes in S_1 and S_2 should be attributed to the insignificant alteration of the base strength when the loading time increases. Under the optimized loading time, propylene dimerization was

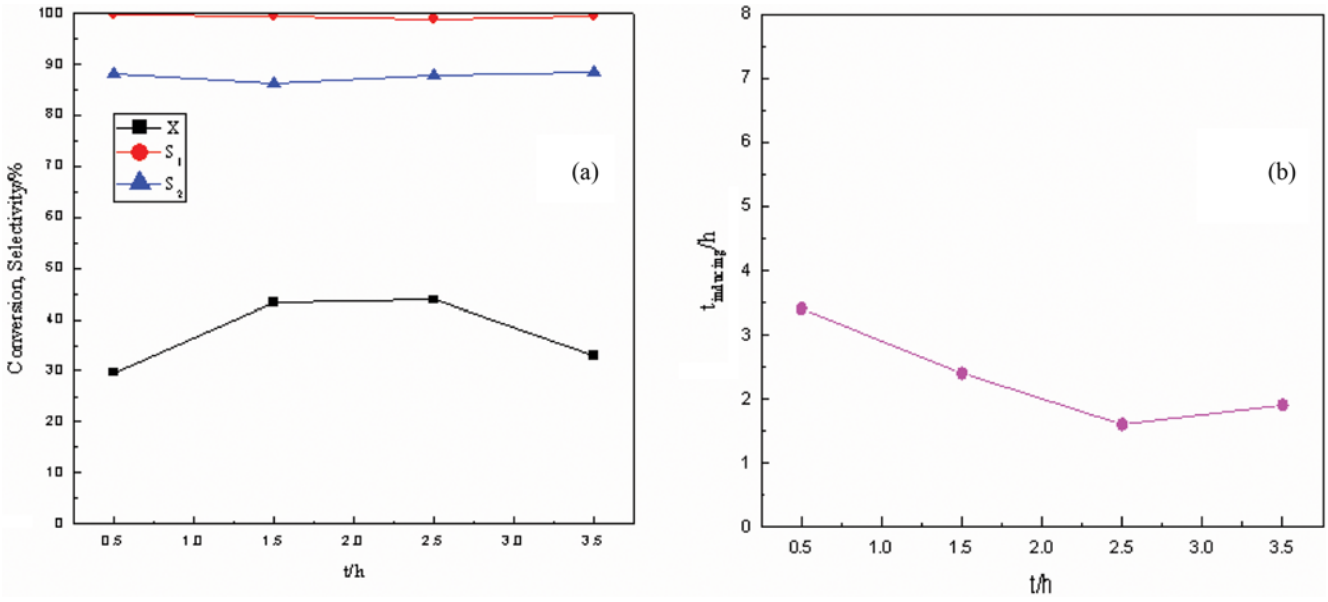

Fig. 5. Effect of alkali metal loading time on the catalytic properties (the samples were prepared by employing the carrier of 120, on which 3.0 wt% of potassium was respectively supported under the temperature of 150 °C).

Table 1. The species and contents of product obtained under optimized loading time

Species	Contents/%	
4-Methyl-1-pentene	84.9	By weight
4-Methyl-2-pentene	4.9	
2-Methyl-1-pentene	0.6	
2-Methyl-2-pentene	0.9	
n-Hexene	6.0	
C9	2.7	

carried out at 150 °C for 20 h. The hexene analysis by gas chromatography is listed in Table 1.

2-2. Effect of the Loading Temperature

The effect of the loading temperature on conversion (X), inducing period ($t_{inducing}$), dimers selectivity (S_1) and 4 MP1 selectivity (S_2) is shown in Fig. 6. With an increase in the loading temperature, X decreased and $t_{inducing}$ progressively increased. A high temperature can facilitate the fast dispersion of metal K and prompt the coalescence of particulates on the carrier. The results in Fig. 6 indicate that the latter predominates during the loading process. The decrease in X can be attributed to a decrease in the quantity of basic sites, which results from the coalescence of surface microcrystals. However, S_1 and S_2 hardly vary with loading temperature, which indicates that the average base strength of the catalyst did not significantly change with temperature. Under the optimized loading time and loading temperature, the propylene dimerization was carried out at 150 °C for 20 h. The hexene product had the composition listed in Table 2.

2-3. Effect of the Metal Loading Amount and Carrier Size

Fig. 7 shows the effects of the metal loading amount and carrier size on the conversion (X), inducing period ($t_{inducing}$), dimer selectivity (S_1) and 4MP1 selectivity (S_2). In Fig. 7, X substantially increases

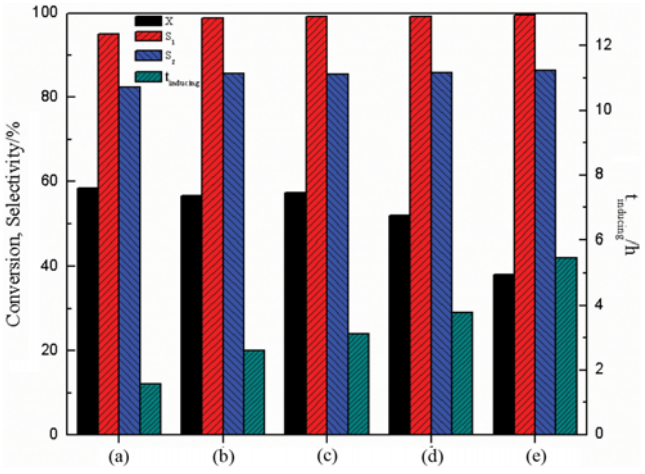

Fig. 6. Effect of loading temperature on the catalytic properties ((a) Loading at 90 °C for 1.5 h; (b) loading at 90 °C for 0.5 h and then at 150 °C for 1 h; (c) loading at 150 °C for 1.5 h; (d) loading at 150 °C for 0.5 h and then at 210 °C for 1 h; (e) loading at 210 °C for 1.5 h (3.8, of potassium was loaded on the carrier with the average size of 120 μm during the total loading time of 1.5 h under certain temperature).

Table 2. The species and contents of product obtained under optimized loading time and temperature

Species	Contents/%	
4-Methyl-1-pentene	86.6	By weight
4-Methyl-2-pentene	5.3	
2-Methyl-1-pentene	0.8	
2-Methyl-2-pentene	1.2	
n-Hexene	4.7	
C9	1.4	

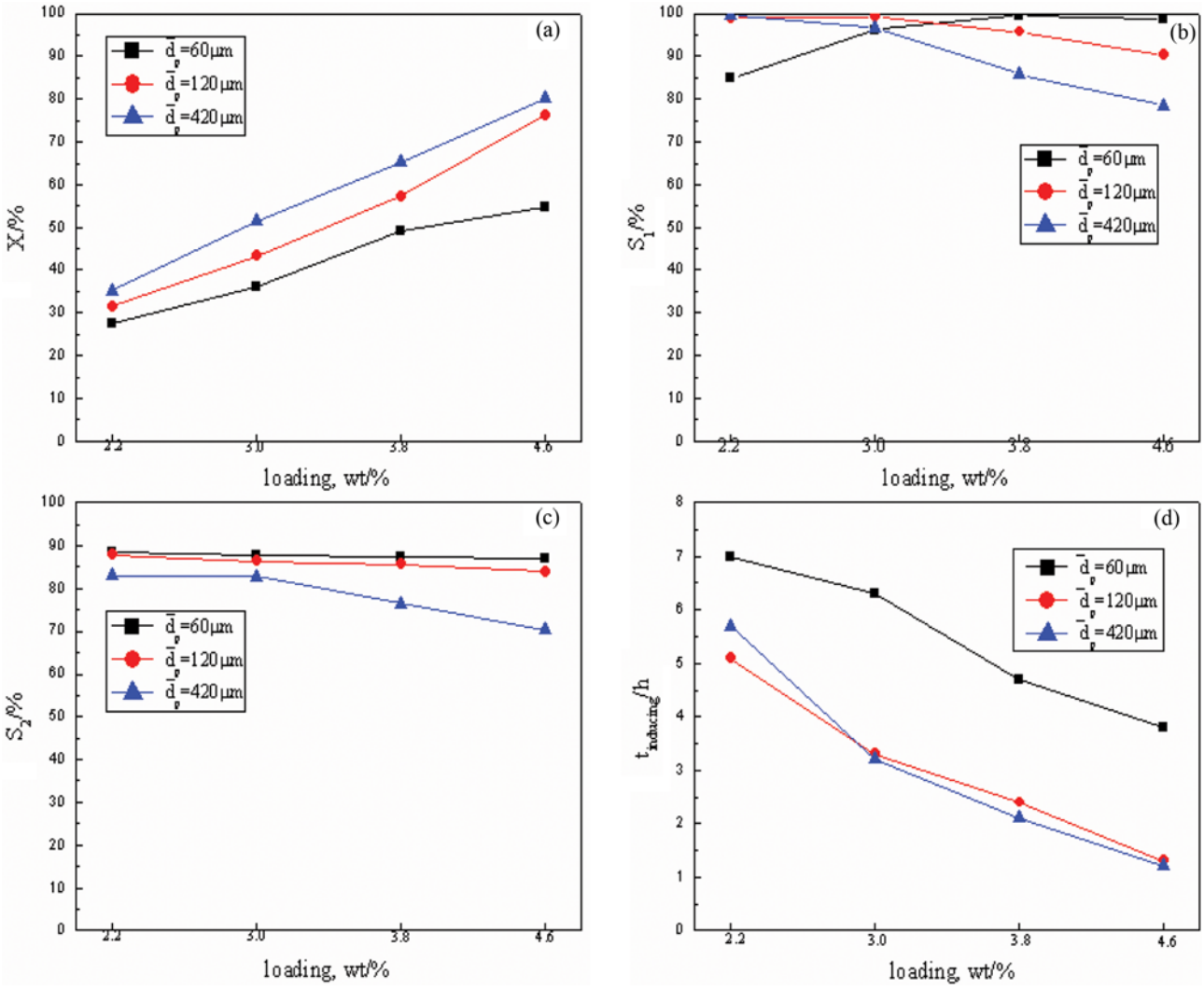

Fig. 7. Effect of alkali metal loading amount and average carrier size of K_2CO_3 on the catalytic properties (the samples were prepared at 150 °C for 1.5 h).

with the increase in the amount of potassium loading and average carrier size, which should result in an increase in the quantity of basic sites. Unlike the surface catalysis of other metal-supported catalysts, the dimerization of propylene may occur throughout a certain depth of the alkali metal on the catalyst [15]. Moreover, a thicker carrier probably benefits the formation of such a structure and enhances the activity. S_1 and S_2 exhibit notable variations in Fig. 7. Under the conditions of a high loading amount and a thin carrier or a low loading amount and a thick carrier, S_1 remains at nearly 100%, as shown in (B) of Fig. 7. This result indicates that the size of the dispersed particulate on the carrier is sufficiently suitable, neither too large nor too small, to optimize S_1 to nearly 100%. (C) in Fig. 7 shows that S_2 drastically decreases when the amount of metal potassium loading increases on the carrier with an average size of 420 μm. This result shows that if the size of the surface particulates on the carrier does not exceed a certain limit, S_2 remains high. According to the results, S_1 and S_2 should be optimized by modifying the base strength, which originates from the change in size of the surface particulates. (D) in Fig. 7 illustrates that $t_{inducing}$ continually shortens when the metal loading amount increases. Additionally, with increasing carrier size, $t_{inducing}$ decreases at the initial the reaction period and then tends to be steady. Considering the microcosmic property of the catalyst, the increase of the carrier size and metal loading amount has a substantial benefit on the growth of the metal microcrystal dispersed on the carrier surface, which can greatly improve the catalytic activity of the catalyst [29]. Under optimized catalyst preparation conditions (including loading time, loading temperature, the metal loading amount and carrier size), propylene dimerization was carried out at 150 °C for 20 h. The hexenes obtained are listed in Table 3.

According to (A), (B), (C), and (D) of Fig. 7, X increased rapidly with the loading amount of alkali metal increases from 2.2 wt% to 4.6 wt%. Alternately, S_1 and S_2 remained high when the loading amount of alkali metal was lower than 3 wt%, but when loading increased to more than 3 wt% alkali metal, S_1 and S_2 decreased, apparently because of the thick metal particle size dispersed on the carrier, which can accelerate the selectivity to oligomerization of propylene. It has been difficult to distill 4MP1 to a high purity com-

Table 3. The species and contents of product obtained under optimized catalyst preparation conditions

Species	Contents/%	
4-Methyl-1-pentene	88.0	By weight
4-Methyl-2-pentene	4.5	
2-Methyl-1-pentene	0.5	
2-Methyl-2-pentene	0.7	
n-Hexene	6.0	
C9	0.3	

mercially. Therefore, even if obtained at a moderate conversion of propylene, a high selectivity to 4MP1 is desirable for industrial application. The catalyst prepared here by dispersing 3 wt% potassium on potassium carbonate was capable of propylene dimerization to 4MP1.

CONCLUSIONS

(1) The metal potassium that was dispersed on potassium carbonate resulted in a new solid superbase of K/K_2CO_3, which exhibits high activity for the dimerization of propylene. The preparation conditions of loading temperature, loading time, metal loading amount and carrier size were studied. The optimal conditions are as follows: loading time of 1.5 h, loading temperature of 150 °C, loading amount of 3 wt% and average carrier size of 120 μm. Because of its loading amount of 3 wt%, the catalyst can be denoted as $3\%K/K_2CO_3$.

(2) The solid superbase catalyst $3\%K/K_2CO_3$ has the highest base strength possible of $H_- \geq 37$, and the concentration of basic sites of $H_- \geq 35$ is approximately 0.3 $mmol \cdot g^{-1}_{CAT}$, which is sufficiently high to abstract the α-H of propylene to form an active intermediate. The catalyst surface of $3\%K/K_2CO_3$ was highly dispersed with the metal K, microcrystalline and exhibited a large specific surface area, which can lead to high conversion.

(3) The super basic sites on K/K_2CO_3 appear to be composed of oxygen species that are adjacent to lattice defects, such as crystalline corners, edges and vacancies of metallic potassium microcrystals, which are highly dispersed on the carrier. Electrons are transferred from the microcrystalline K metal to the conjoint oxygen atom, which enhances the electron density and improves the capability of donating electron pairs and accepting hydrogen protons to form super basic sites.

REFERENCES

1. Y. R. Wang and Z. H. Jing, *China Synthetic Resin and Plastics*, **27**, 71 (2010).
2. P. Dahal, J. H. Kim and Y. C. Kim, *Korean J. Chem. Eng.*, **31**, 1 (2014).
3. J. B. Wilkes, in *Proceedings of the 7th World Petroleum Congress*, **5**, 399 (1967).
4. O. Yoshio and H. Hideshi, *Solid base catalysis*, Springer, Berlin Heidelberg (2011).
5. Y. D. Wei, S. D. Zhang and G. S. Li, *Chinese J. Catal.*, **32**, 891 (2011).
6. G. Suzukamo, M. Fukao and M. Minobe, *Chem. Lett.*, **16**, 585 (1987).
7. K. Tanaka, H. Yanashima, M. Minobe and G. Suzukamo, *J. Appl. Surf. Sci.*, **121-122**, 461 (1997).
8. H. Matsuhashi and K. J. Klabunde, *Langmuir*, **13**, 2600 (1997).
9. H. Matsuhashi, M. Oikawa and K. Arata, *Langmuir*, **16**, 8201 (2000).
10. R. M. Bota, K. Houthoofd, P. J. Grobe and P. A. Jacobs, *Catal. Today*, **152**, 99 (2010).
11. L. R. M. Martens, P. J. Grobet, W. J. M. Vermeiren and P. A. Jacob, *Stud. Surf. Sci. Catal.*, **28**, 935 (1986).
12. N. Yasuo, A. Yusaku and K. Ryoko, *J. Phys. Chem. Solids*, **73**, 1538 (2012).
13. N. Takehito, T. Hajime and H. Atsufumi, *Phys. Rev. B*, **88**, 1 (2013).
14. R. M. Schramm, US Patent, 2,968,488 (1961).
15. J. M. Fuchs, M. Gallot and L. Saussine, European Patent, 0,291,411 (1992).
16. J. B. Wilkes, *Organ. Chem.*, **32**, 3231 (1967).
17. J. B. Wilkes, US Patent, 3,175,020 (1965).
18. J. B. Wilkes, US Patent, 3,216,947 (1965).
19. J. K. Hambling, *Chemistry in Britain*, **5**, 354 (1969).
20. J. K. Hambling and R. P. Northcott, *Rubber and Plastics*, **49**, 224 (1968).
21. J. K. Hambling, UK Patent, 933,253 (1961).
22. C. A. Drake, US Patent, 4,595,787 (1986).
23. C. A. Drake, US Patent, 5,057,639 (1986).
24. Z. S. Yuan, *Refining and Chemical Industry*, **12**, 10 (2001).
25. M. K. Mitsuo, US Patent, 4,388,480 (1983).
26. M. S. Zhang, L. Ke, J. Yang, Y. Feng and L. M. He, *Petrochem. Technol.*, **1**, 737 (2002).
27. A. W. Shaw and C. W. Bitter, *Organ. Chem.*, **30**, 3286 (1965).
28. V. R. Ansheles and I. I. Pis'man, *Russ. Chem. Rev.*, **46**, 620 (1977).
29. J. R. Anderson, *Structure of metallic catalysts*, Academic Press, New York (1975).
30. Y. C. Xie, N. F. Yang, Y. J. Liu and Y. Q. Tang, *Sci. China Chem. (Series B)*, **26**, 337 (1983).
31. D. Lin, *Chinese J. Inorg. Chem.*, **2**, 250 (2000).